APPLICATION OF A RIGID BODY IMPACT MODEL TO THE PEDESTRIAN - CAR COLLISION

by

D.P. Wood, B.E., M.Eng.Sc., Ph.D., C.Eng., M.I.E.I.
Wood & Associates
25/26 St. Mary's Abbey
Dublin 7
Ireland

1. INTRODUCTION

This paper uses a simple model for the pedestrian, that of a single segment rigid body. The author (1) has previously applied this model of the pedestrian to the vehicle impact speed and pedestrian throw distance relationship and obtained correlation with experimental throw distance results. Here the model is specifically applied to the impact phase between the pedestrian and the car. This is considered as two discrete events, primary impact with the front of the car and secondary impact between the pedestrian's head and the car. The calculated results from the model are compared with published results of cadaver and dummy tests.

2. IMPACT MODEL

Figure 1 shows the representation of the primary and secondary impacts. The primary impact is between the front of the car and the pedestrian. As the pedestrian's c.g. is above the top of the front edge of the bonnet the upper contact point at the front edge of the bonnet is taken as being the location of the primary impact. The geometric relationship between the primary and secondary impact points is represented by a straight line of angle α. Analysis shows that,

$$V_{ph}/V_{ci} = \frac{M_c.k^2}{k^2(M_c+M_p)+M_c.h^2} \qquad 1$$

$$V_r/V_{ci} = \frac{M_c.h^2}{k^2(M_c+M_p)+M_c.h^2} \qquad 2$$

$$\omega/V_{ci} = \frac{M_c.h}{k^2(M_c+M_p)+M_c.h^2} \qquad 3$$

$$V_{pv}/V_{ci} = \frac{h.b_w.M_c}{k^2(M_c+M_p)+M_c.h^2} \qquad 4$$

Equation 2 shows after primary impact that the pedestrian has a relative horizontal velocity V_r , towards the car. The magnitude of this relative velocity depends upon the height, h ,of the pedestrian's c.g. above the contact point, the relative velocity increasing with h . The pedestrian to car mass ratio,M_p/M_c, also influences the relative velocity, with the relative velocity reducing as the mass ratio increases.

Equation 3 shows that the magnitude of the pedestrian's rotational velocity ω , towards the car is primarily dependent on h , the height of the pedestrian's c.g. above the topmost contact point on the front of the bonnet. The primary impact gives the pedestrian an upward velocity, equation 4. In addition to depending on the value of h , the magnitude of this upward velocity is related to the horizontal distance from the contact point on the pedestrian to the pedestrian's c.g.b_ω . A pedestrian side impact will result in a significantly higher upward velocity than that obtained when the pedestrian is hit to the front or back as the value of b_ω is significantly higher to the side.

The attitude of the pedestrian at impact also influences the magnitude of the velocity as the radius of gyration of the pedestrian is less about the transverse axis. The difference in the values is small, in the order of 6 1/2 percent (2). Comparison between a pedestrian impacted on the side and on the front/back shows that a pedestrian hit on the front/back will after primary impact have;

a slightly lower horizontal velocity V_{ph} ,
a significantly lower upward vertical velocity V_{pv} ,
a slightly higher rotational velocity ω ,
a slightly higher relative horizontal velocity towards the car V_r ,

than a pedestrian hit on the side.

From this comparison the model infers that the secondary impact for a pedestrian hit on the front/back will take place after a shorter time interval and when the pedestrian's body has rotated through a smaller angle than when the impact occurs on the pedestrian's side. Also the pedestrian's head will be further onto the car and the velocity at which the head impacts the car will be higher.

3. SECONDARY IMPACT

The model assumes that the secondary impact takes place between the pedestrian's head and the vehicle upper surface.

The equations for the secondary impact are most readily expressed in terms of θ, the angle of the body from the vertical when secondary impact takes place. The time from primary impact to head contact is,

$$t_{hc} = \left[2 \left\{ \frac{(b_w - h\tan\alpha)\theta + h + b_w\tan\alpha - d_h\tan\alpha\sin\theta + d_h\cos\theta}{g(1+\mu_c\tan\alpha)} \right\} \right]^{1/2} \qquad 5$$

Where α is the angle between the upper contact point on the front of the car and the head contact point. The velocity of the car immediately before impact expressed in terms of θ and t_{hc} is,

$$V_{ci} = \frac{\theta\,(k^2(M_c+M_p)+M_c h^2)}{h.M_c\,t_{hc}} \qquad 6$$

The location of the centre of the head contact can be expressed in terms of the horizontal distance from the primary contact point, C_h and the ratio of wrap round distance to pedestrian height, W.R. ratio,

$$C_h = h\theta + (d_h - h_w)\sin\theta - \tfrac{1}{2}\mu_c.\,g\,t_{hc}^2 - b_w \qquad 7$$

$$\text{W.R. RATIO} = \frac{d_b + C_h\,(1+\tan\alpha^2)^{1/2}}{P_h} \qquad 8$$

The horizontal, vertical and total velocities at which the head strikes the car are,

$$V_{rh}/V_{ci} = \frac{M_c.h(h+d_h\cos\theta)}{k^2(M_c+M_p)+h^2M_c} - \frac{\mu_c\,g\,t_{hc}}{V_{ci}} \qquad 9$$

$$V_{rv}/V_{ci} = \frac{M_c.h(d_h\sin\theta - b_w)}{k^2(M_c+M_p)+h^2M_c} + \frac{g\,t_{hc}}{V_{ci}} \qquad 10$$

$$V_t/V_{ci} = \left(\frac{V_{rh}^2}{V_{ci}^2} + \frac{V_{rv}^2}{V_{ci}^2} \right)^{1/2} \qquad 11$$

With the terms containing μ_c equations 5, 7 and 9 include the effect of uniform vehicle deceleration.. When there is no braking until after secondary impact the terms containing are ignored. The effect of vehicle pitch is included by adjusting the values of α and h .

4. TIME TO HEAD CONTACT

Severy (5) carried out tests using dummies. Figure 2 compares his experimental results for adult dummy impacts with a Plymouth car and the calculated contact time - impact velocity relationship. The calculated curve matches the experimental results.

5. HEAD IMPACT VELOCITY

Cesari et al (4,5) have published the results of 58 cadaver and 43 dummy tests using Citreon Visa and Citreon GSA cars. These tests were carried out for both side and front impacts to the pedestrian. Figure 4 compares the calculated head impact velocity - car impact velocity ratio, V_t / V_{ci} for a pedestrian height of 1.67 m with the experimental cadaver results for impact to the side. The calculated values are similar in magnitude to the experimental results but are on average biased towards higher values than those obtained experimentally. Figure 3 shows the corresponding results for impacts to the front. In this case the calculated results are similar to the experimental results but in general are lower than the experimental results.

6. HEAD CONTACT POINT

Figures 5 and 6 compare the calculated wrap round ratios for front and side impacts using a pedestrian height of 1.67m with the results obtained by Cesari (4,5). The calculated wrap round ratios are similar to the experimental results but the average experimental values are higher than the calculated curves.

7. EFFECT OF VEHICLE BRAKING

During braking cars adopt a dive attitude due to load transfer effects. Braking dive reduces the height of the front of the bonnet and increases the bonnet angle. Figure 7 shows the effect. For cars which have identical front and rear axle suspension bounce frequencies the changes in bonnet height and angle are;

$$\Delta d_b = -\frac{(W.B.(1-F.A.)+\theta_h)\mu_c g h_c}{W_b^2 . W.B^2 (1-F.A.) F.A.} \quad 12$$

$$\tan(\Delta\alpha) = \frac{\mu_c g h_c}{W_b^2 W.B^2 (1-F.A.) F.A.} \quad 13$$

When the front and rear bounce frequencies are not the same there will be a change in the height of the car's centre of gravity. However this effect is small and can be ignored.

Figure 8 compares the difference between an unbraked and braked car (braking 7.85 m/s^2, μ_c = 0.8) for a representative pontoon shaped car. With braking of 7.85 m/s^2 the front of the bonnet drops by 0.1m and the bonnet angle increases by 2.1°. Figure 8 shows that the head contact time, t_{hc} is shorter for the braked condition. There is no significant difference between the predicted head impact velocities for the two conditions.

Comparison of the distance to head contact, C_h shows that at low speeds the effect of braking is to bring the head contact point close to the front of the car. As the impact speed is increased the head contact point moves rapidly backwards. At speeds above 7 m/s the head contact point is closer to the windscreen under the braked condition than for the unbraked condition. The model indicates that at high speeds the head contact point continues to move backwards for the braked condition. For the unbraked condition the head contact distance, C_h reaches a maximum at 10 m/s and then slowly decreases, moving back towards the front of the car.

8. HIGH SPEED IMPACTS

Grandel et al (6) published the results of staged impacts between dummies and Ford Taunus and V.W. Passat cars for both the braked and unbraked conditions at speeds between 15.0 m/s and 24.4 m/s (33.5 m.p.h. and 54.6 m.p.h.). For the unbraked Ford Taunus (speed 15.0 m/s) they showed that the head impact occurred on the bonnet in front of the windscreen. When the vehicle is braked (speeds 15.0 m/s and 18.33 m/s) the impact location moves backwards to the lower windscreen area. For the unbraked V.W. Passat (speed 23.1 m/s) the impact occurred in the upper windscreen area.

Figures 9 and 10 show the calculated results for the Ford Taunus and V.W. Passat respectively. For the V.W. Passat the model gives a lower head contact position, at base of windscreen compared with the upper windscreen for the experimental tests. The calculated head contact times

for the Taunus are slightly higher than the experimental results. The calculated head contact positions are closer to the front of the car than the experimental results. However the calculations confirm the experimental findings that the head contact position for the unbraked car is closer to the front of the car than for the braked vehicle and that at high speeds the movement of the head contact point diminishes and that consequently head impact with the windscreen is not inevitable.

9. DISCUSSION

The comparisons between the published results of staged impact tests with both cadavers and dummies and the model show that the results obtained from the single segment pedestrian model for time to head contact, head contact position and head impact velocity are comparable with the test results and that the trends found in tests are also shown by the model.

The calculated head contact positions are, in general, closer to the front of the cars than the experimental results. This difference is due to the fact that the primary impact between the pedestrian and the front of the car takes a short but measurable period of time during which there is relative movement of the pedestrian towards the windscreen. The relative motion has not been included in the model.

The model indicates for impact with an unbraked car that the head contact position is substantially independent of impact speed for speed above 7 m/s.

The experimental results from Cesari et al (4.5) show that there is a high variability in the head impact velocity. Modelling of the pedestrian factors contributing to this variability can only be obtained when any multisegment pedestrian models such as that developed by van Wijk (7). The analytical model presented in this paper is such that the fundemental sensitivity of the head contact point, and impact velocity to pedestrian and vehicle parameters can be readily determined and assessed. The model is restricted in representation of the head contact point by a secant line. Representation of the actual profile of a car requires numerical solution of the equations. This can be readily carried out on microcomputer.

10. REFERENCES

1. Wood D.P. 'Impact and Movement of Pedestrians in Frontal Collisions with Vehicles' Proceedings Institution Mechanical Engineers Vol 202 No. D2,

51/88.

2. Reynolds H.M. 'The Inertial Properties of the Body and its Segments' in NASA (1978), Anthropometric Source Book. NASA Defence Publication No. 1024. Vol. I.

3. Severy D.J. 'Auto-pedestrian Collision Experiments' SAE paper 660080, 1966.

4. Cesari D, et al 'Experimental Study of Pedestrian Kinematics and Injuries' Proceedings of the Fifth International IRCOBI Conference on the Biomechanics of Impacts 1980 p273 - 285.

5. Cesari D, et al ' Analysis of Pedestrian Head Kinematics based on Car-Pedestrian Test Results' Proceedings of the International IRCOBI conference 1985 p139 - 158.

6. Grandel J. et al 'Kinematics and Head Injuries in Vehicle / Pedestrian Accidents at Speeds above 50 KPH' Proceedings International IRCOBI Conference on The Biomechanics of Impacts 1986 p189 - 204.

7. van Wijk, J., et al 'MADYMO pedestrian simulations'. Proceedings of SAE Symposium on Pedestrian impact, injury and assessment, 1983 P - 121 paper 830060 p 109 - 117.

11. NOTATION

b_w Half width (depth) of pedestrians body.
P_h Height of pedestrian.
d_h Distance from c.g. of pedestrian to top of head.
h Distance between upper contact point at front of car and c.g. of pedestrian.
k Radius of gyration of pedestrian about horizontal axis.
h_w Distance from top of head to centre of head.
g Gravitational acceleration.
M_p Mass of pedestrian.
M_c Mass of car.
$F.A.$ Proportion of static weight of car on front axle.
O_h Horizontal distance from front axle to contact point on front of car.
ω_b Natural frequency of car in bounce.
d_b Vertical height to contact at front of car.
t_{hc} Time between primary and secondary impacts;
V_{ci} Velocity of car at primary impact.

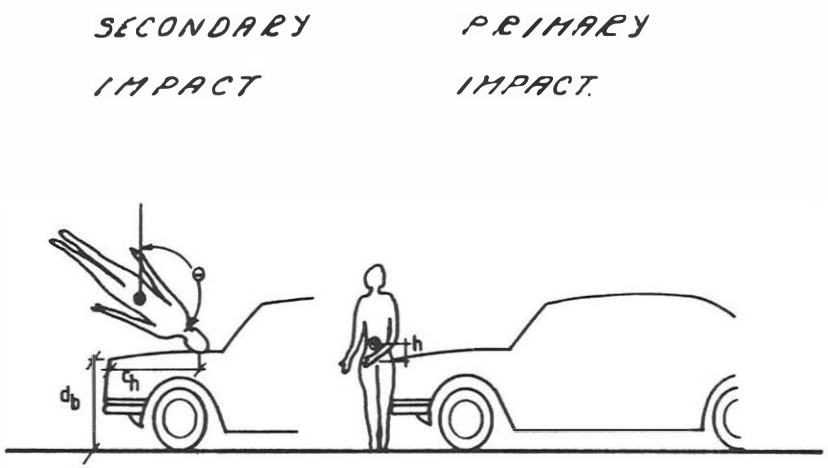

FIGURE 1 : REPRESENTATION OF PRIMARY AND SECONDARY IMPACTS.

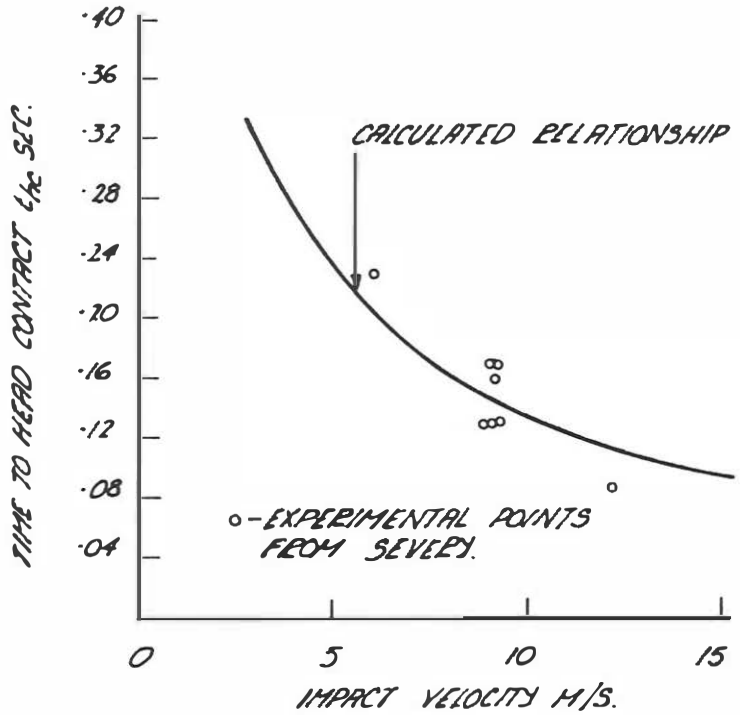

FIGURE 2 : COMPARISON OF CALCULATED TIME TO HEAD IMPACT 4/4 SEC WITH EXPERIMENTAL DUMMY TESTS BY SEVERY (3).

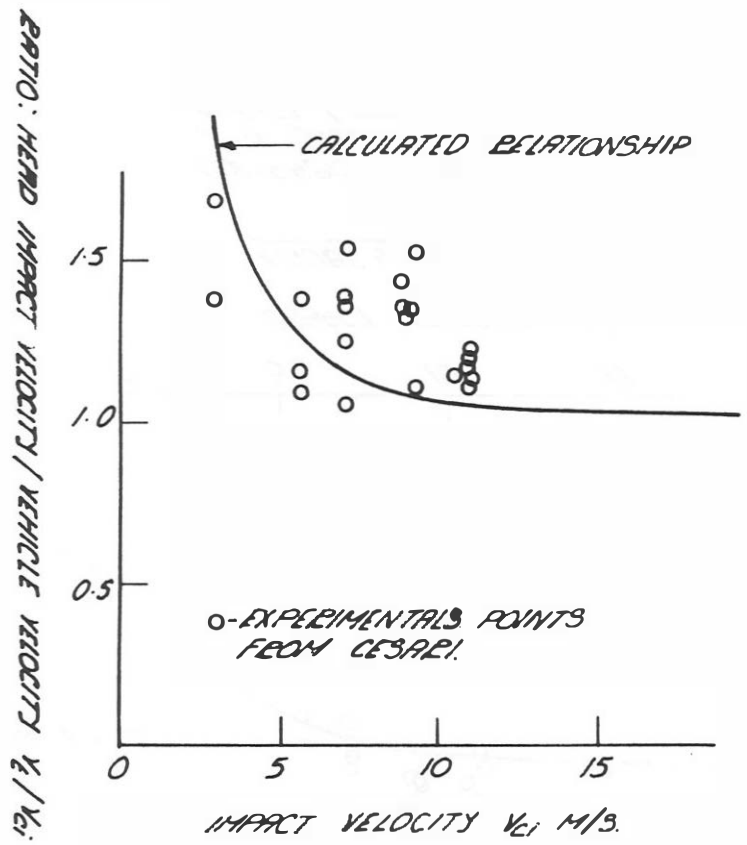

FIGURE 3 FRONTAL IMPACT

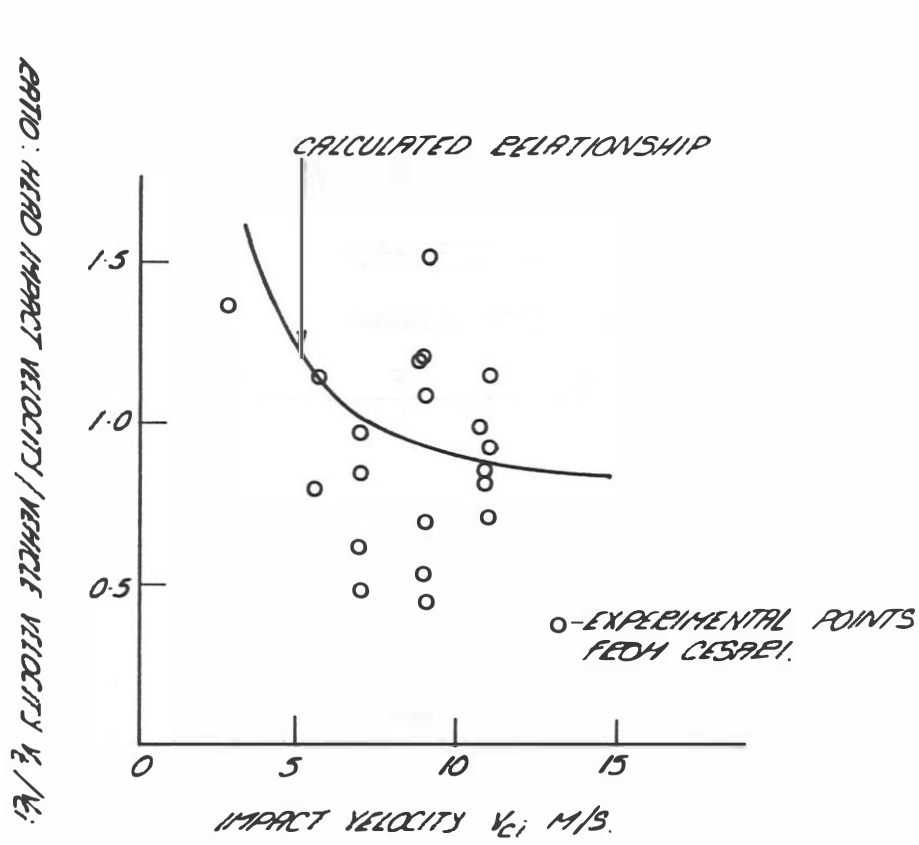

FIGURE 4 SIDE IMPACT.

COMPARISON BETWEEN CALCULATED HEAD IMPACT VELOCITY / VEHICLE VELOCITY RATIOS AND CADAVER TESTS USING CITREON GSA AND CITREON VISA CARS (FROM CESARI (4, 5)).

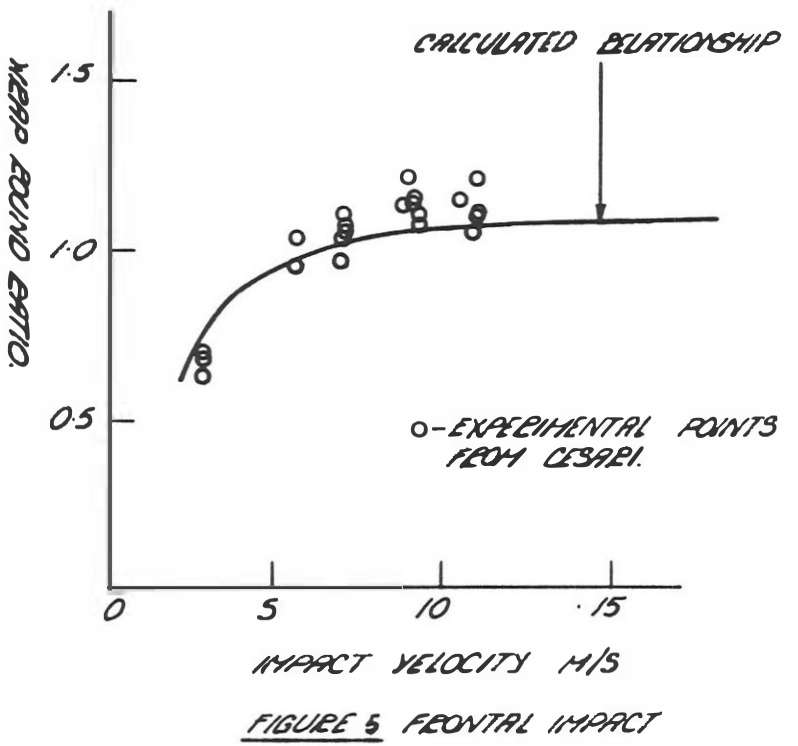

FIGURE 5 FRONTAL IMPACT

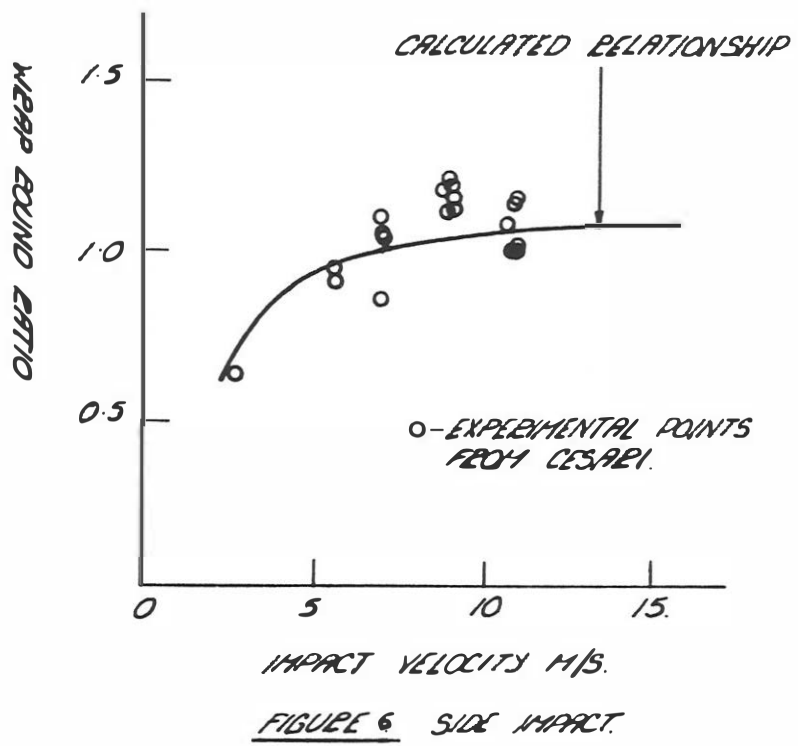

FIGURE 6 SIDE IMPACT.

COMPARISON BETWEEN WRAP ROUND RATIOS OBTAINED FROM STAGED IMPACTS WITH CITREON VISA AND CITREON BSA CARS USING CRAPVEES WITH CALCULATED CURVES (FROM CESARI (4,5)).

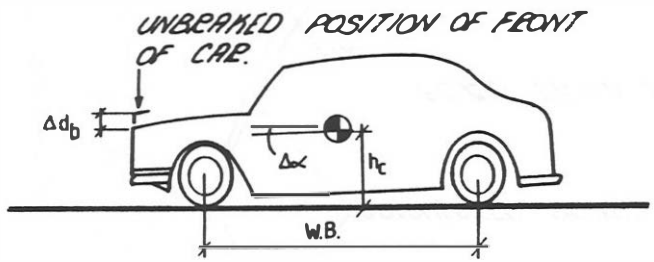

FIGURE 7: ATTITUDE OF BRAKING CAR.

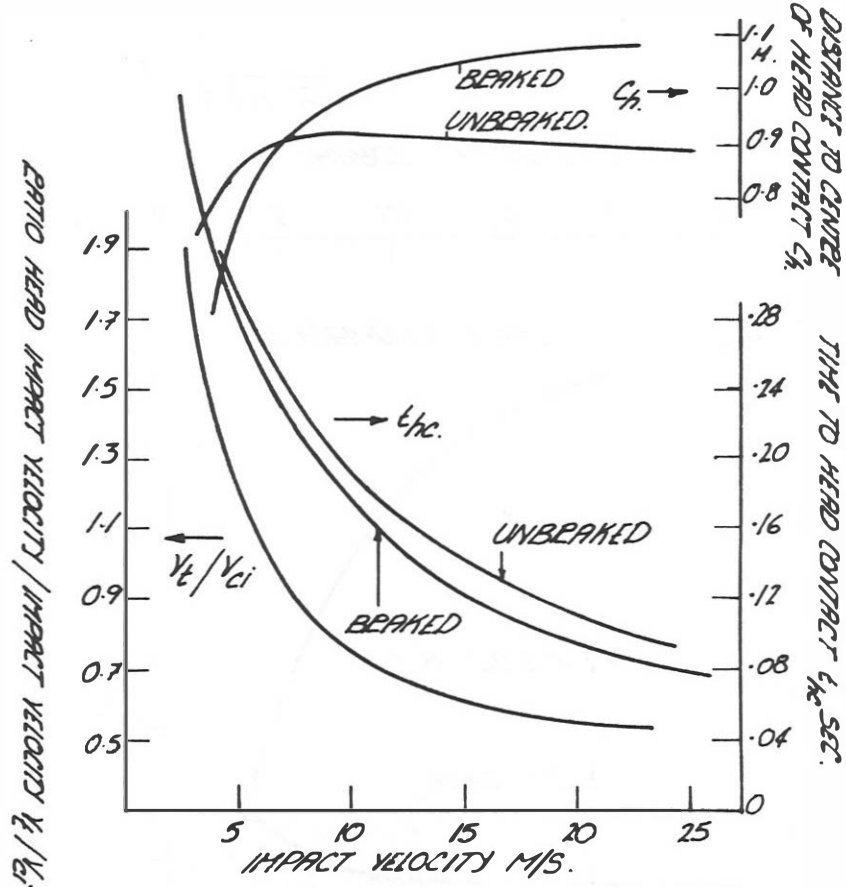

$M_p/M_c = 0.06$, $P_h = 1.7M$, $d_h = 0.73M$,
$h_c = 0.53M$, $O_h = .94M$, W.B. $= 2.44M$, $W_b = 1.25$ Hz.

FIGURE 8: THEORETICAL ANALYSIS OF EFFECT OF BRAKING FOR TYPICAL "PONTOON" CAR ON PEDESTRIAN SIDE IMPACTS.

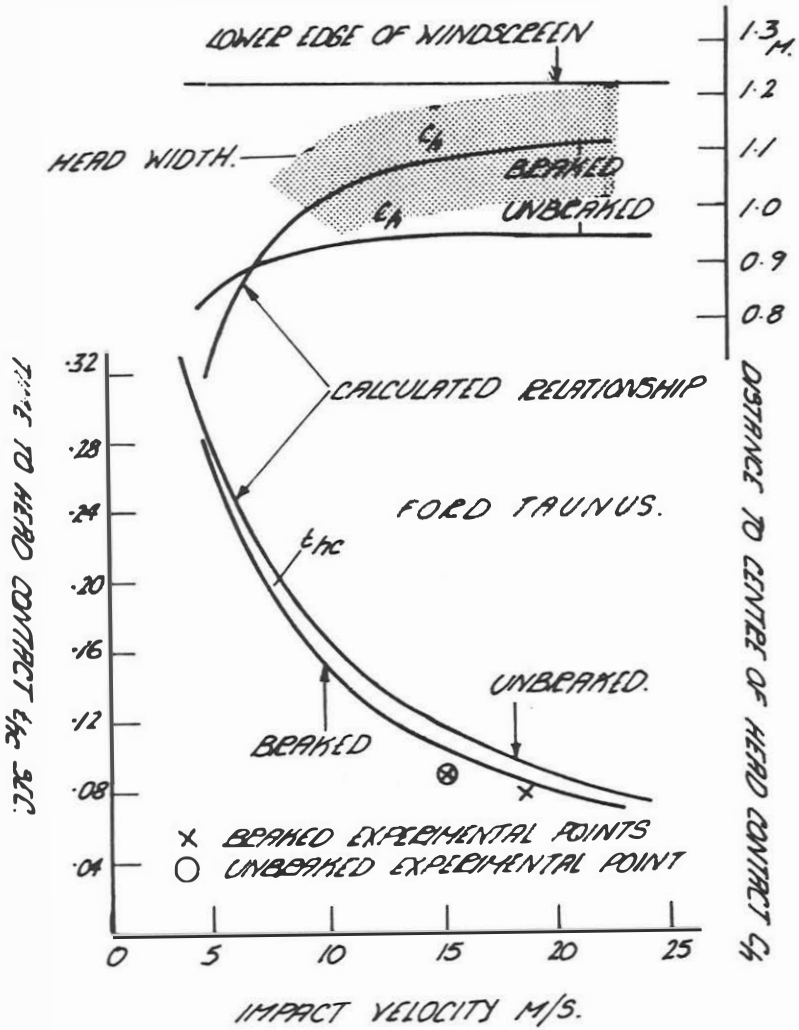

FIGURE 9. COMPARISON BETWEEN CALCULATED RELATIONSHIPS AND HIGH SPEED DUMMY TESTS FROM BRANDEL (6).

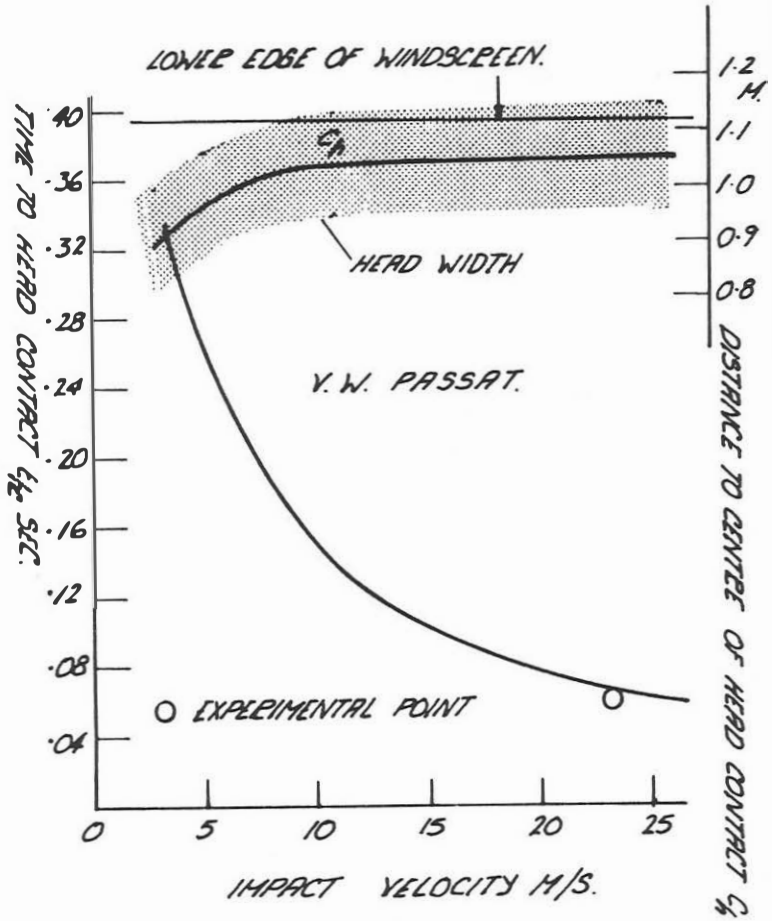

FIGURE 10.